Low thresholds for a nonconventional polymer blend-Amplified spontaneous emission and lasing in $F8_{1-x}$

Hassan, Muhammad Umair; Liu, Yee Chen; Butt, Haider; Hasan, Kamran ul; Chang, Jui Fen; Olawoyin, Ayooye Abigael; Friend, Richard Henry

DOI:
10.1002/polb.23947

Low Thresholds for a Nonconventional Polymer Blend – Amplified Spontaneous Emission and Lasing in $F8_{1-x}:SY_x$ System

M. U. Hassan[1, 2][§], Yee-Chen Liu[2]*, H. Butt[3], Kamran ul Hasan[4], Jui-Fen Chang[5], Ayooye Abigael Olawoyin[1] and R. H. Friend[1]*

[1]Center for Micro and Nano Devices, COMSATS Institute Information Technology, Shehzad Town, Park Road, Islamabad, 44000, Pakistan

[2]Cavendish Laboratory, University of Cambridge, JJ Thomson Avenue, Cambridge, CB3 0HE, United Kingdom

[3] Microengineering and Nanotechnology Laboratory, School of Mechanical Engineering, University of Birmingham, Birmingham, United Kingdom

[4]Department of Science and Technology, Campus Norrköping, Linköping University, Bredgatan 34, SE-601 74 Norrköping, Sweden

[5]Department of Optics and Photonics, National Central University, Chung-Li, 32001, Taiwan

[§]Corresponding Author's E-mail: muhammad_umair@comsats.edu.pk

[*]Authors having equal contribution in this work

Keywords: (polymer laser, amplified spontaneous emission, optical pumping, low optical threshold)

Abstract

A mixture of two polymer materials, poly (9,9-dioctylfluorene) (F8), and one of the poly (*para*-phenylenevinylene) derivatives, superyellow (SY) have been used to make $F8_{1-x}:SY_x$ polymer blend system. Under a 3-5 ns pulsed-laser excitation, this system shows excellent optical properties with low threshold values of ≈ 14 μJ-cm^{-2} and ≈ 8 μJ-cm^{-2} for amplified spontaneous emission (ASE) and optically pumped lasing (OPL), respectively. The proposed system is also electroluminescent and an interesting candidate for future research on polymer injection lasers.

Introduction

Realization of charge conduction and optical properties in semiconducting polymers[1] have evoked strong interest in understanding their physics,[2] development of new materials with improved properties[3] and utilization of these properties in electrical and optical applications. These materials offer great advantages of easy solution-based processablity,[4] mechanical flexibility[5] and low-cost fabrication of large-area devices.[6,7] As a result, polymer-based devices such as field effect transistors,[8,9] light emitting diodes (LEDs)[4] and photovoltaic cells[10,11] are rapidly securing their place in the market in parallel with their inorganic counterparts. Polymer materials can be designed to have high photoluminescence (PL) quantum efficiencies,[12] large stimulated emission cross-sections,[13] and a wide emission range across the visible spectrum,[14,15] which open up the quest for using them as gain-media for optical amplifiers and laser applications.[15,16] Particularly, fluorene based polymers such as Poly(9,9-dioctylfluorene-alt-benzothiadiazole) (F8BT),[5] poly (9,9-dioctylfluorene) (F8)[17] and poly(*para*-phenylenevinylene) (PPV) derivatives such as Super-Yellow (SY)[18] have been investigated for this purpose. Low lasing thresholds , $I_L \approx 36$ nJ-cm^{-2} have been achieved in poly[9,9-dioctylfluorene-alt-9,9-di(4-methoxy-phenyl)fluorine (F8DP) under optically excitation.[19] However, lasing in polymer based electrical devices still remains a challenge which is limited due to the lack of combination of suitable electrical and optical properties in a single gain media.[14]

Various methods have been investigated to increase the optical-gain of polymers, such as patterning,[19] blending of different materials,[20] and using different experimental conditions.[17] These methods offer great improvements and provide directions for further exploration. For example 2D distributed feedback (DFB) have edge over 1D-DFB in terms of achieving low

lasing thresholds.[18] A femtosecond pulsed pump beam also serves the same purpose and has advantage over a nanosecond laser excitation.[21] Another technique is Förster resonance energy transfer (FRET), in which energy transfer takes place between a guest and a host material resulting in the increase of optical gain.[22] In this technique, devices are fabricated by carefully blending two polymers and using the blend as an emissive layer.[20,23] This method has already made a considerable success in improving optically pumped lasing but, little in injection lasing. Therefore there is strong need of a single gain medium which can show a low threshold for lasing under optical excitation as well as high current-density in electrical devices such as in polymer LEDs.[14,24]

In this paper, we study amplified spontaneous emission (ASE) and optically pumped lasing (OPL) in a mixture of two polymer materials, F8 and SY, which give us a new blend-system, $F8_{1-x}$:SY_x, where x represents the weight ratio of the blended constituents. We choose $F8_{1-x}$:SY_x because a) both polymer systems, F8 and SY, are already well-understood and extensively reported in the literature.[12,25] b) there is a large spectral overlap between F8 emission and SY absorption, as given in **Figure 1**, which play very important role in FRET, and c) there is a large gap between the absorption spectrum of F8 and emission spectrum of SY, which reduces the optical losses caused by self-absorption. Therefore, an efficient FRET is possible, and there is potential for lowering the ASE and OPL thresholds. $F8_{1-x}$:SY_x based polymer-LEDs also exhibit excellent luminous efficiency. This combination of excellent electrical and optical properties makes the system a potential candidate for future research on polymer injection lasers.

We achieve low thresholds for ASE, $I_A \approx 14$ μJ-cm^{-2} and OPL, $I_L \approx 8$ μJ-cm^{-2} for $F8_{0.9}$:$SY_{0.1}$, under a pulsed laser excitation with pulse rate, t = 3-5 ns, and wavelength,

λ = 407 nm. Compared with conventional blend systems such as $F8_{1-x}$:$F8BT_x$[26] and TFB_{1-x}:$F8BT_x$[4] in which polymers from same polyfluorene (PF) group are mixed, $F8_{1-x}$:SY_x (F8 from PF and SY from PPV group) proves to be a better system in terms of its optical and electrical properties. This combination in a single gain medium is a crucial parameter for realizing polymer injection laser. [14] Here, we shall mainly deal only with optical excitation experiments – systematic evolution of diode efficiency with changing SY concentration in F8 matrix will be dealt in detail in a separate report.

Results and Discussion

Two types of optical devices were investigated for ASE and OPL, respectively. The device schematics and their respective characterization setups are respectively shown in **Figure 2a**, **b**. Both types of devices were optically excited by a pump pulsed laser having λ = 407 nm, t = 3–5 ns, and repetition rate, f = 10 Hz. For ASE, asymmetric waveguides had quartz / $F8_{1-x}$:SY_x (~ 200 nm)/ air configuration. The waveguides were excited by the pump-beam of a perfectly flattop intensity profile, ~ 100 μm × 4 mm, achieved by placing a cylindrical lens in the beam path and the spectra was collected at the edge as shown in **Figure 2a**. For OPL, $F8_{1-x}$:SY_x films of ~ 200 nm thickness were deposited on silicon-dioxide (SiO_2) 1D-DFB resonators. These devices were excited by a pump beam of circular profile with a diameter of ~ 220 μm, obtained by placing a convex lens in the beam path and the spectra was collected at almost normal to the device-plane as shown in **Figure 2b**.

Our investigation began with the ASE study of $F8_{1-x}$:SY_x system for different SY concentrations, x = 0.05, 1, 0.1, 0.2, 0.3, 0.75, 0.95, respectively, see **Figure 3a**. For low pump intensities, $I_P < I_A$, the emission spectra of the pumped stripe is essentially the normal PL spectra for all

values of x. As soon as ASE kicks in at $I_P \geq I_A$, most of the light gets highly amplified before emitting out of the edge of the pumped stripe region. The amplified vibronic peak starts appearing in the broad spectra having its centers at the maximum of the net gain spectrum.[27]. We observe ASE peaks at $\lambda_{A(x = 0)} \approx 451$ nm and $\lambda_{A(x = 1)} \approx 581$ nm for $x = 0$ (pure F8 films) and $x = 1$ (pure SY films), respectively, with a difference of $\Delta\lambda_A \approx 130$ nm between the two peaks. Upon adding small amount of SY, $x = 0.1$, a large red shift, $\Delta\lambda_A > 100$ nm, is observed compared with $\lambda_{A(x = 0)}$. Although, there is 90% of F8 (by weight) present in this composition ($F8_{0.9}$:$SY_{0.1}$), F8 shows its negligible appearance such that whole spectra shifts towards the longer wavelengths, and resembles more like that for pure SY. Strong suppression of F8 signature is attributed as an indication of efficient FRET in $F8_{1-x}$:SY_x,which is seen even for very small values of x. With every increase in SY concentration, the ASE peak generally undergoes a red-shift with increased value of I_A, as shown in **Figure 3a**, **b**, respectively. The values for I_A are determined by plotting the PL output intensities against the pump pulse energy and recognized by a sudden rise at $I_P = I_A$, [27]. We obtain $I_A \approx 28$ μJ-cm^{-2} and ≈ 106 μJ-cm^{-2} for $x = 0$ and 1, respectively, which are in good agreement with the literature.[17,28] The lowest threshold value, $I_A \approx 14$ μJ-cm^{-2}, is observed for $x = 0.1$. It is noted that $x = 0.05$ also shows the threshold value comparable with that for $x = 0.1$, the PL output however remains low with an additional peak at ≈ 451 nm in the PL emission region for F8 (i.e. the highest gain 0-1 peak). We believe that low PL output for low SY concentrations, $x < 0.1$, is mainly because of the competition between the gain spectra of F8 and SY.[29] Another important observation is that the output intensities for large concentrations, $x > 0.2$, also level-off with increase in the pump intensities. This is because of the exciton-exciton annihilation (EEA), which suppresses the ASE at large pump intensities and has already been reported for PPVs.[30, 31] EEA is considered to be the main loss channel

which becomes stronger for larger SY concentrations. The redshift for increased SY concentration is also associated with aggregate formation which generally results interchain interaction at lower energies.[31, 32] It is notable that these results are repeatable: the output intensities do not change under identical pump conditions in repeated experiments. This infers that the leveling-off of the output intensities for large pump intensity for different values of *x* is mainly because of EEA and not caused by the photo-degradation of the material. These cells were saved under N_2 environment and tested again after one year: we found no appreciable change in the results depicting good stability of the proposed blend system. **Figure 3c** shows the curves between output intensity and stripe length, *l*, for $F8_{0.9}$:$SY_{0.1}$ waveguides excited under three different pump powers. The ASE gain coefficient, *g*, was determined by fitting data using relationship $I = I_p \times A[\exp(g \times l) - 1]/g$,[15] We obtained considerably large value of gain coefficient, $g \sim 37$ cm^{-1} for $x = 0.1$. The saturation of the curves is noticed at large stripe lengths. This was not because of photo degradation of the film as repeated experiments gave the similar results. Nevertheless, the gain saturation can occur because of extreme amplification while light travels through the waveguide which results in depletion of substantial fraction of the excitons.[15] Atomic force microscopy was used to study the morphology of the blend system. No preferred architecture or lateral phase separation across the entire range of samples was observed, see inset of **Figure 3c** for $x = 0.1$. Therefore, light scattering effects, if any, due to the phase separation are not considered significant here and are beyond the scope of this paper.

After obtaining the best results for $x = 0.1$ for ASE, $F8_{0.9}$:$SY_{0.1}$, is selected for optically pumped lasing experiments. Although, there are concerns while estimating the refractive index for planar waveguides especially for materials having broad absorption spectra,[33] here, we adopted a simple approach: we use the Bragg expression to calculate the DFB period, Λ, i.e.

$m\lambda_L = 2\, n_{eff} \times \Lambda$, where, m is the diffraction order, λ_L gives the lasing wavelength, and n_{eff} is the effective refractive index of the film. Using the second-order diffraction, $m = 2$, $\lambda_L \approx 555$ nm and $n_{eff} \approx 1.6$, we decided to fabricate a 1D-DFB grating with $\Lambda = 345$ nm. As a second check, we used finite element method to simulate 2D wave propagation in the device of $\Lambda = 345$ nm in two conditions, when a) the grating is placed in air and, b) a material with refractive index, $n \approx 1.6$, is deposited on the grating, as shown in **Figure 4a**, **b**. The transmission spectra simulated for both the transverse electric (TE) and transverse magnetic (TM) modes of the incident light are shown in **Figure 4a**. Photonic band gaps (regions where no wave propagation through the lattice takes place) are observed in the simulated transmission spectra, as displayed in **Figure 4b**. The band gap around $\lambda \approx 400$ nm – 550 nm is observed for air which undergoes a red-shift when air is replaced with a material with $n = 1.6$, resulting in a stop-band of $\lambda \approx 550$ nm – 650 nm. Based on the characterization and simulation results a 1D-DFB is prepared and OPL experiments are performed after obtaining film of $F8_{0.9}$:$SY_{0.1}$ on the DFB. The results are shown in **Figure 4c** and **4d**. For small pump energies below the lasing threshold, $I_P < I_L$, normal PL spectra is noticed at the output, except a Bragg-dip centered at $\lambda_B \approx 545$ nm. This dip appears because of the effective band gap (as discussed above) induced by the grating which blocks the propagation of the waveguided photons.[34] With increase in the pump energy above lasing threshold, $I_P > I_L$, the lasing occurs near the center of the Bragg-dip where a narrow peak at $\lambda_L \approx 545$ nm with full width half maximum, $\Delta\lambda_{1/2} \approx 2$nm, dominates the spectrum, as shown in **Figure 4c**. It is notable that there is an offset of ~ –10 nm in λ_L compared with initial calculations. Also, the position of the lasing peak lies slightly below the lower band-edge estimated in the simulations. To resolve this, it is speculated that there might a change in n_{eff} casing this shift. To confirm this, simulations are again performed for a lower refractive index, $n \approx 1.5$, which results in a blue-

shifted band gap (around $\lambda \approx 525$ nm – 600 nm) compared with that for $n \approx 1.6$. It is notable that the experimental lasing peak now lies within the stop-band, as shown in **Figure 4b** and **c**. To confirm our speculation of change in n_{eff}, we use another 1D-DFB with $\Lambda = 335$ nm. For this, the lasing peak shifts at $\lambda_{\text{L}} \approx 530$ nm, as shown in **Figure 4c**. By using the Bragg's expression for both grating periods and lasing peaks, we obtain a value of $n_{eff} \approx 1.58$. One of the possible reasons for this change can be the local heating caused by the pump-beam. The lasing thresholds values, $I_P = I_{\text{L}}$, are determined by the rapid increase in the output intensity when plotted against pump intensity. We obtained $I_{\text{L}} \approx 8$ μJ-cm^{-2} and 50 μJ-cm^{-2} for $\Lambda = 345$ nm and $\Lambda = 335$ nm, respectively. It is proposed that these values can still be lowered significantly by optimizing the experimental techniques. For example, using 2D -DFB, tuning the DFB period, exciting with faster pump-beam (with a femtosecond pulsed laser) and using optimized pump-wavelength (high F8 absorption) would further lower the lasing threshold.[21,18,34] For a summary of ASE and OPL experiment, see table 1.

The detailed evolution of optical properties and time resolved exciton dynamics (subject of a separate report) show that the major pathway for thresholds lowering in the proposed blend system is indeed via remarkably efficient FRET mechanism, wherein, the calculated Förster radius is about 4.3 to 6.3 nm and F8 exciton decay life time (@ 450 nm) severely reduces from ~ 413 ps to ~ 288 ps for x = 0.1. However, at low SY concentrations, dilution assisted decrease in threshold from SY molecules cannot be ruled out as less exciton-exciton and self-quenching are expected.[31] This also augments the high optical efficiency of the proposed system.

In summary, we have proposed a new polymer blend system, $F8_{1-x}$:SY_x, which shows excellent electro-optical properties. It exhibits efficient energy transfer via FRET mechanism

which takes place between F8 host to SY guest molecules, low lasing threshold value being $< 8\ \mu J\text{-}cm^{-2}$ under nanosecond pulsed laser excitation for 1D DFB have been realized – optical excitation with shorter pulses, 2D DFBs, and shorter wavelength will further lower the threshold. The blend system also shows excellent performance when used as emissive layer in polymer LEDs. We believe that the combination of optical and electrical properties of $F8_{1-x}:SY_x$ make this system interesting for future research on advanced device architectures such as polymer injection lasing.

Experimental

Asymmetric waveguides (quartz / $F8_{1-x}:SY_x$ / air): Quartz substrates were obtained from UQG Optics Ltd. After receiving, the substrates were cleaned in an ultrasonic bath with acetone and isopropanol (10 minutes each). F8 (294 kg-mole^{-1}, Cambridge Display Technology) and SY (616 kg-mole^{-1}, Merck) were dissolved in chlorobenzene to form $F8_{1-x}:SY_x$ solutions. $F8_{1-x}:SY_x$ films were deposited by spin coating of this solution onto the cleaned quartz substrates in nitrogen environment. Subsequently, these films were dried on a hotplate at 70℃ for 30 minutes, and shifted to the testing setup for amplified spontaneous emission. The thickness of the films was about 200 nm.

Lasing Devices: Lasing devices were fabricated by spin coating the $F8_{0.9}:SY_{0.1}$ solution on silicon-dioxide 1D DFB gratings. After spin coating, the drying process was performed on hotplate at 70℃ for 30 minutes in a nitrogen glovebox. The DFB gratings with periods of 345 nm and 335 nm and depth of 70 nm were prepared on a Si/SiO_2 substrate by using e-beam patterning.

Optical Pumping: Both types of devices were optically excited with laser pulses of 3 – 5 ns (10 Hz) obtained from a compact housing of the nanosecond optical parametric oscillator (OPO) system and Nd:yttrium aluminum garnet (Nd:YAG) Q-switched laser (NT342B series, EKSPLA). The pump wavelength was set to 407 nm. The cylindrical lens was placed in the pump beam path to obtain a rectangular stripe of ~ 100 μm × 4 mm with a perfectly flattop intensity profile for ASE experiment. Whereas, a pump beam with a spot size of ~ 220 μm (in diameter) was illuminated on DFB waveguides for OPL experiments.

Acknowledgments

The authors wish to acknowledge Bodo Wallikewitz for very useful discussion and providing DFBs and Cambridge Display Technology for providing F8.

References

[1] J. H. Burroughes, D. D. C. Bradley, A. R. Brown, R. N. Marks, K. Mackay, R. H. Friend, P. L. Burns, A. B. Holmes, *Nature* **1990**, *347*, 539–541.

[2] R. H. Friend, R. W. Gymer, A. B. Holmes, J. H. Burroughes, R. N. Marks, C. Taliani, D. D. C. Bradley, D. A. D. Santos, J. L. Bredas, M. Logdlund, W. R. Salaneck, *Nature* **1999**, *397*, 121–128.

[3] B. K. Yap, R. Xia, M. Campoy-Quiles, P. N. Stavrinou, D. D. C. Bradley, *Nature Materials* **2008**, *7*, 376–380.

[4] J.-S. Kim, P. K. H. Ho, C. E. Murphy, R. H. Friend, *Macromolecules* **2004**, *37*, 2861–2871.

[5] B. Wenger, N. Tétreault, M. E. Welland, R. H. Friend, *Applied Physics Letters* **2010**, *97*, 193303–193303–3.

[6] S. Brittain, K. Paul, X.-M. Zhao, G. Whitesides, *Physics world* **n.d.**, *11*, 31–36.

[7] S.-C. Chang, J. Bharathan, Y. Yang, R. Helgeson, F. Wudl, M. B. Ramey, J. R. Reynolds, *Applied Physics Letters* **1998**, *73*, 2561–2563.

[8] J. Zaumseil, R. H. Friend, H. Sirringhaus, *Nat Mater* **2005**, *5*, 69–74.

[9] L.-L. Chua, J. Zaumseil, J.-F. Chang, E. C.-W. Ou, P. K.-H. Ho, H. Sirringhaus, R. H. Friend, *Nature* **2005**, *434*, 194–199.

[10] J. J. M. Halls, C. A. Walsh, N. C. Greenham, E. A. Marseglia, R. H. Friend, S. C. Moratti, A. B. Holmes, *Nature* **1995**, *376*, 498–500.

[11] J. Nelson, *Science* **2001**, *293*, 1059 –1060.

[12] R. Gupta, M. Stevenson, A. J. Heeger, *Journal of Applied Physics* **2002**, *92*, 4874–4877.

[13] U. Scherf, S. Riechel, U. Lemmer, R. . Mahrt, *Current Opinion in Solid State and Materials Science* **2001**, *5*, 143–154.

[14] N. Tessler, *Advanced Materials* **1999**, *11*, 363–370.

[15] I. D. W. Samuel, G. A. Turnbull, *Chemical Reviews* **2007**, *107*, 1272–1295.

[16] G. Heliotis, D. D. C. Bradley, G. A. Turnbull, I. D. W. Samuel, *Applied Physics Letters* **2002**, *81*, 415–417.

[17] M. H. Song, D. Kabra, B. Wenger, R. H. Friend, H. J. Snaith, *Advanced Functional Materials* **2009**, *19*, 2130–2136.

[18] E. B. Namdas, M. Tong, P. Ledochowitsch, S. R. Mednick, J. D. Yuen, D. Moses, A. J. Heeger, *Advanced Materials* **2009**, *21*, 799–802.

[19] C. Karnutsch, C. Pflumm, G. Heliotis, J. C. deMello, D. D. C. Bradley, J. Wang, T. Weimann, V. Haug, C. Gärtner, U. Lemmer, *Applied Physics Letters* **2007**, *90*, 131104–131104–3.

[20] R. Xia, G. Heliotis, D. D. C. Bradley, *Applied Physics Letters* **2003**, *82*, 3599–3601.

[21] C. Bauer, H. Giessen, B. Schnabel, E. -B Kley, C. Schmitt, U. Scherf, R. F. Mahrt, *Advanced Materials* **2001**, *13*, 1161–1164.

[22] T. Förster, *Discussions of the Faraday Society* **1959**, *27*, 7–17.

[23] T. Virgili, D. G. Lidzey, D. D. C. Bradley, *Advanced Materials* **2000**, *12*, 58–62.

[24] N. Tessler, N. T. Harrison, D. S. Thomas, R. H. Friend, *Applied Physics Letters* **1998**, *73*, 732–734.

[25] M. Berggren, A. Dodabalapur, R. E. Slusher, Z. Bao, *Nature* **1997**, *389*, 466–469.

[26] A. Cadby, R. Dean, A. M. Fox, R. A. L. Jones, D. G. Lidzey, *Nano Letters* **2005**, *5*, 2232–2237.

[27] M. D. McGehee, R. Gupta, S. Veenstra, E. K. Miller, M. A. Díaz-García, A. J. Heeger, *Physical Review B* **1998**, *58*, 7035–7039.

[28] B. H. Wallikewitz, D. Hertel, K. Meerholz, *Chemistry of Materials* **2009**, *21*, 2912–2919.

[29] R. Gupta, M. Stevenson, M. D. McGehee, A. Dogariu, V. Srdanov, J. Y. Park, A. J. Heeger, *Synthetic Metals* **1999**, *102*, 875–876.

[30] G. Denton, N. Tessler, N. Harrison, R. Friend, *Physical Review Letters* **1997**, *78*, 733–736.

[31] T.-Q. Nguyen, V. Doan, B. J. Schwartz, *The Journal of Chemical Physics* **1999**, *110*, 4068–4078.

[32] M. U. Hassan, Y. C. Liu, K. ul Hasan, H. Butt, J. F. Chang, R. H. Friend, *Applied Materials Today* **2015,** *1*, 45-51.

[33] G. A. Turnbull, P. Andrew, M. J. Jory, W. L. Barnes, I. D. W. Samuel, *Physical Review B* **2001**, *64*, 125122.

[34] G. Heliotis, R. Xia, G. A. Turnbull, P. Andrew, W. L. Barnes, I. D. W. Samuel, D. D. C. Bradley, *Advanced Functional Materials* **2004**, *14*, 91–97.

[35] M. H. Song, B. Wenger, R. H. Friend, *Journal of Applied Physics* **2008**, *104*, 033107.

Figures

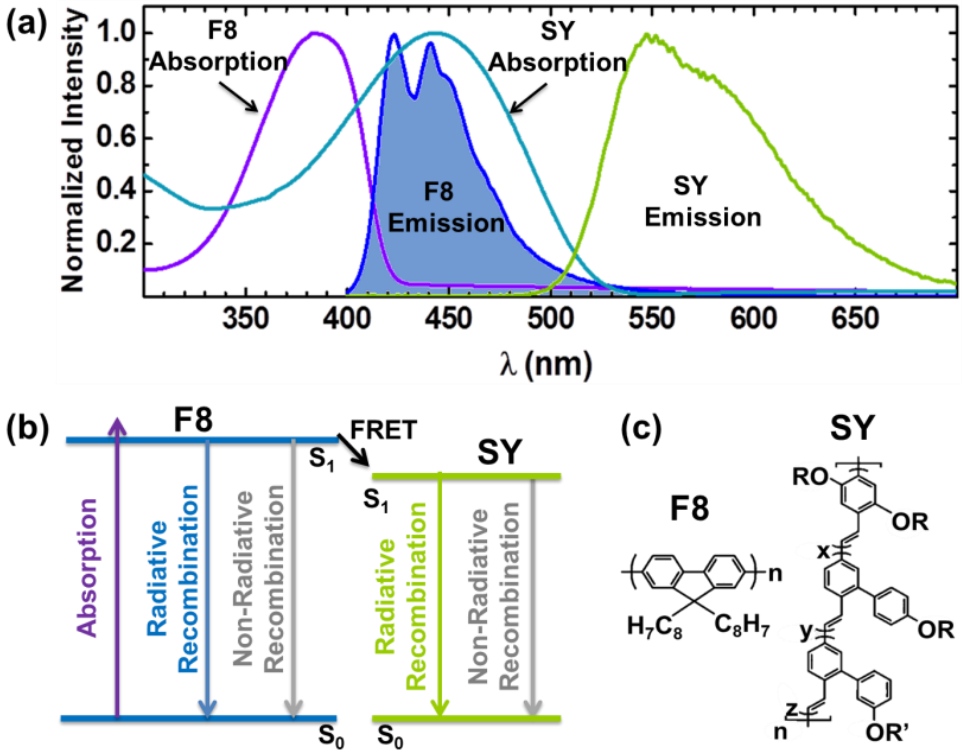

Figure 1. a) Normalized absorption spectra (violet and light-blue solid curves) and PL spectra (blue and green solid curves) of F8 and SY, respectively. The strong overlap of emission and absorption spectra of F8 and SY, respectively causes efficient FRET, lowering the ASE and OPL thresholds, **b)** A brief description of FRET, showing energy transfer from F8 (host) to SY (guest) molecular levels and, **c)** The chemical structures of the F8 and SY molecules.

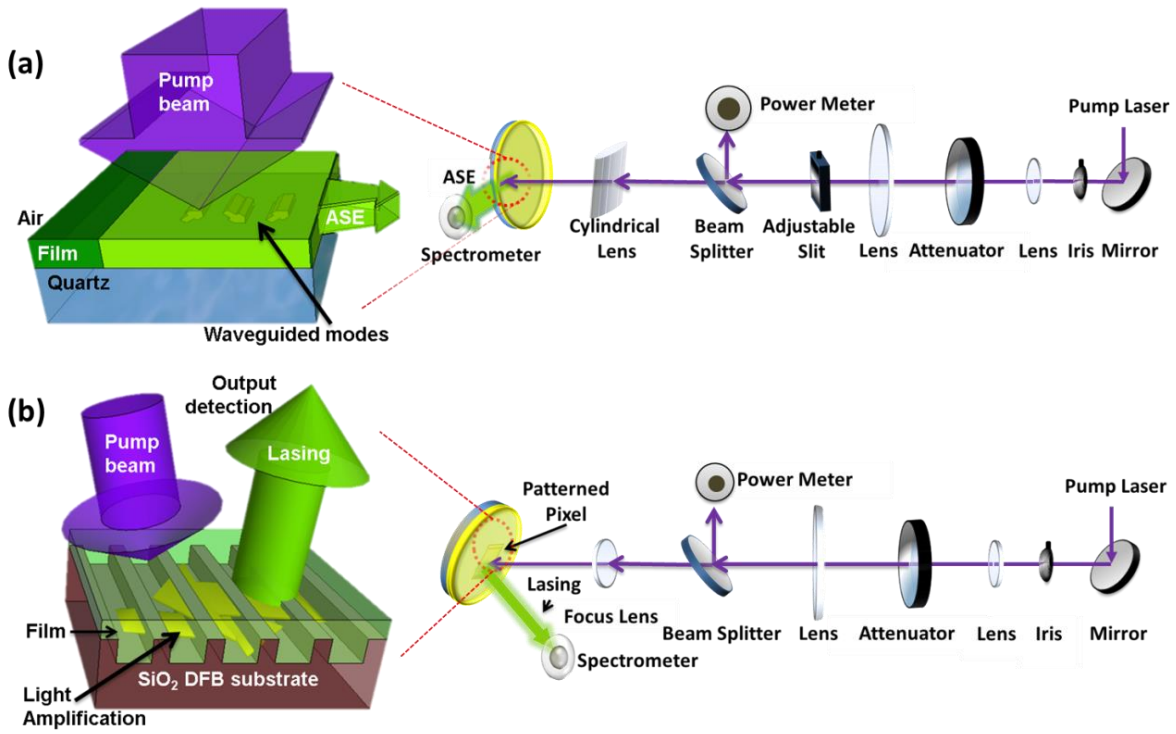

Figure 2. Schematic diagrams for ASE, OPL and their characterization setups: **a)** A rectangular (~ 100 µm × 4 mm) pulsed laser (407 nm, 3 – 5 ns) pump beam was used to excite the asymmetric waveguide devices (quartz / $F8_{1-x}$:SY_x / air), and emission spectra was collected at the edge, **b)** OPL devices ($F8_{1-x}$:SY_x solution-deposited by spin coating on a SiO_2 1D-DFB) were exited with a pulsed laser (407 nm, 3 – 5 ns) pump beam with a spot size of ~ 220 µm in diameter, and the spectra was obtained at normal to the device surface.

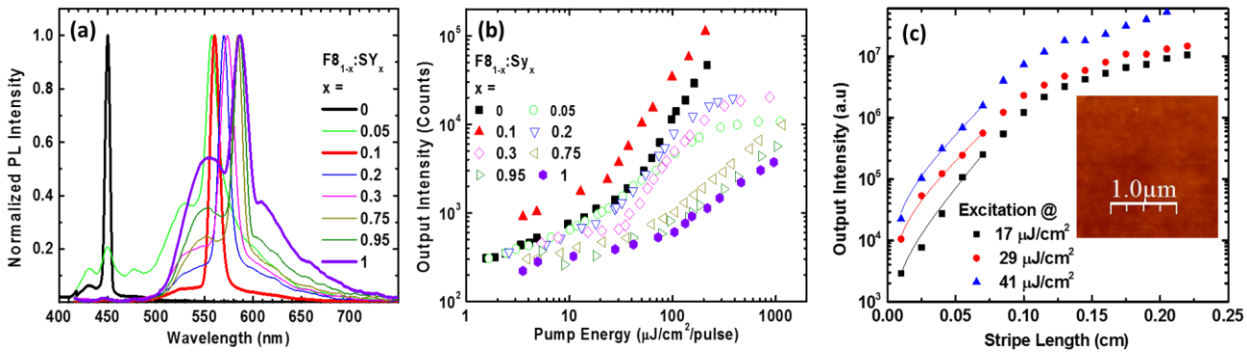

Figure 3. a) Normalized edge-detected PL spectra of the F8$_{1-x}$:SY$_x$ waveguides with increasing SY concentration, taken at pump intensities approximately 10 – 15 times above the thresholds of the corresponding polymer films and normalized to their maximum intensities within the visible range. Addition SY suppresses F8 emission which disappears for small $x \approx 0.1$, indicating efficient FRET. The ASE peaks also red-shift with increasing x because of interchain interaction between SY aggregates. **b)** PL output intensity vs. pump pulse energy for F8$_{1-x}$:SY$_x$ film with increasing value of x: lowest threshold value of $I_A \approx 14\mu J\text{-}cm^{-2}$ was obtained for $x = 0.1$ which is an order of magnitude lower than that for pure SY. **c)** The dependence of emission intensity on the excitation length at different pump intensities for $x = 0.1$. The average gain value obtained was ~ 37 cm^{-1} from the fitting (solid lines). The inset is AFM image of the same concentration which exhibits no preferred architecture or phase separation.

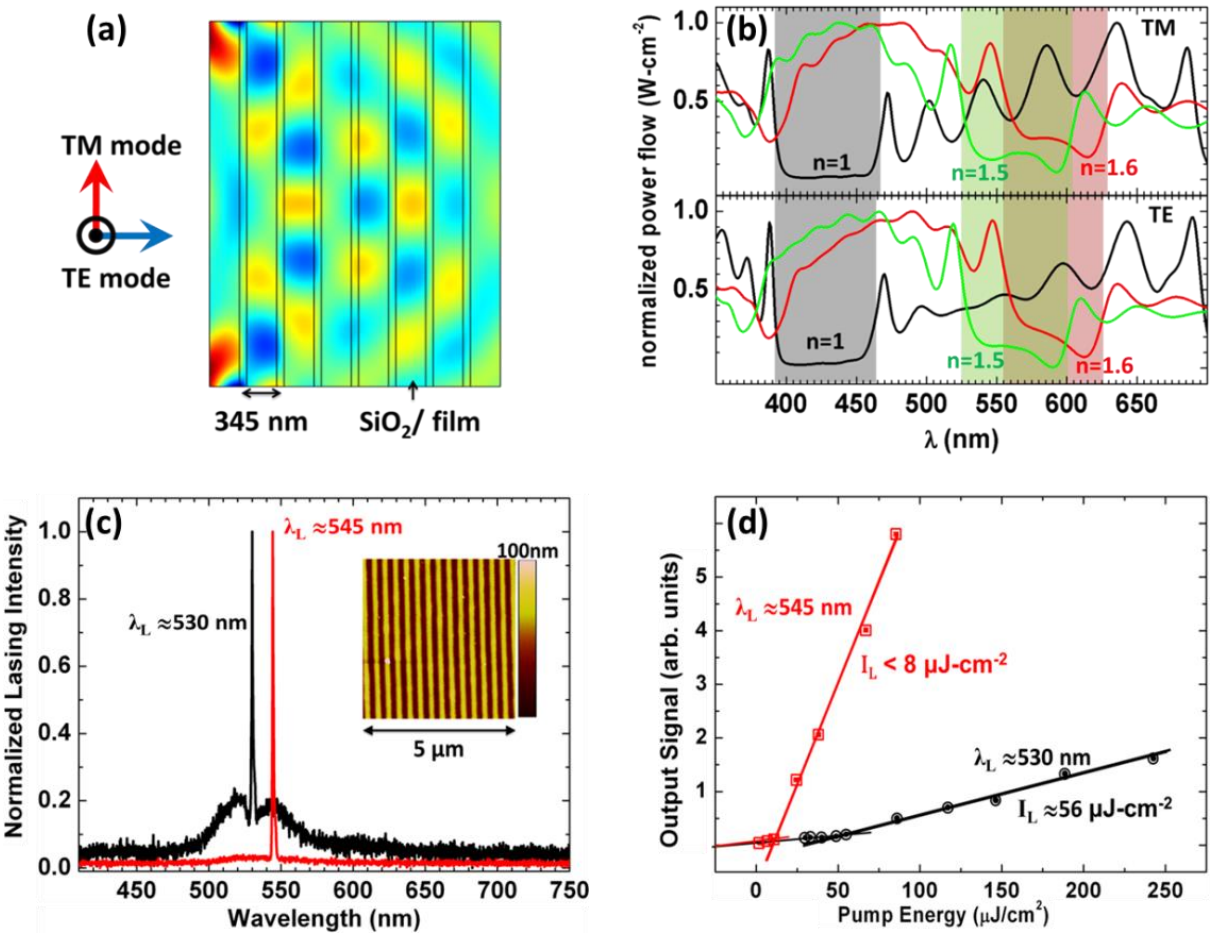

Figure 4. a) Simulated wave propagation of a 800 nm TE mode wave, across the lattice of a 1D photonic crystal, **b)** Simulation of TE and TM mode transmission spectra for the device performed with the index of the surrounding medium as 1, 1.5 and 1.6 and their corresponding bandgaps. **c)** Normalized PL spectrum of OPL devices with $F8_{0.9}$:$SY_{0.}1$ composition and grating period Λ = 330 nm and 345 nm (black and red curves, respectively) resulting in lasing peaks at $\lambda_L \approx$ 530 nm and 545 nm, respectively. The inset is the AFM image of the grating, and, **d)** Laser output pulse energy a function of excitation pulse energy: lasing threshold, $I_L \approx 8$ µJ-cm^{-2} was obtained for Λ = 345 nm.

Table 1. ASE peak wavelength, λ_A, ASE threshold, I_A, and OPL threshold, I_L, for different values of x.

$F8_{1-x}:SY_x$ (x, wt. fraction)	λ_A (nm)	I_A (μJ-cm^{-2})	I_L (μJ-cm^{-2})
0 (pure F8)	451	28	20 for 1D-DFB. 500 *ps pump-pulse* [35]
0.05	553	16	-
0.1	555	14	< 8
0.2	564	32	-
0.3	568	35	-
0.75	578	62	-
0.95	580	93	-
1 (pure SY)	581	106	3.6 for 1D-DFB. *100 fs* pump-pulse[18]